Abdominal Radiology (2019) 44:4048–4056
https://doi.org/10.1007/s00261-019-02155-4

PANCREAS

Differentiation of pancreatic head ductal adenocarcinoma from inflammatory pancreatic pseudomass by MR cholangio-pancreatography: utility of the duct-interrupted, corona, and attraction signs

Kevin Beker[1] · Karen S. Lee[1] · Leo L. Tsai[1] · Tarek Hegazi[1] · Alejandro Garces-Descovich[1] · Alexander Brook[1] · Koenraad J. Mortele[1]

Published online: 27 July 2019

Abstract

Purpose To determine sensitivity and specificity of the "duct-interrupted," "corona," and "attraction" signs on MR cholangio-pancreatography (MRCP) in distinguishing pancreatic head ductal adenocarcinoma (PDAC) from inflammatory pancreatic pseudomass (IPP).

Materials and methods This study included 53 adults (33 men and 20 women, mean age, 55 years; range, 17–87 years) with a pancreatic head mass who underwent MRCP. Three blinded radiologists independently reviewed each MRCP exam and three signs were assessed: (1) the "duct-interrupted" sign, deemed positive for PDAC if the duct within the mass demonstrated complete interruption with upstream dilation; (2) the "corona" sign, considered positive for PDAC if dilated side-branches were located exclusively outside the mass; and (3) the "attraction" sign, deemed positive for IPP if the dilated common bile duct showed attraction and angulation towards the mass. Sensitivity, specificity, and positive and negative predictive values of the signs were calculated, as well as interobserver agreement.

Results Out of 53 masses, 17 (32%) were PDAC and 36 (68%) were IPP. Sensitivity, specificity, and positive and negative predictive values of the "duct-interrupted" sign to differentiate between PDAC from IPP for the three readers were 29–53%, 89–95%, 56–82% and 73–81%, respectively ($\kappa = 0.41$); for the "corona" sign, they were 29–53%, 81–100%, 56–100%, and 75–78%, respectively ($\kappa = 0.4$), and for the "attraction" sign, they were 20–25%, 71–82%, 64–75%, and 31–34%, respectively ($\kappa = 0.54$).

Conclusion The "duct-interrupted" and "corona" MRCP signs have high specificity for diagnosing PDAC, while the "attraction" sign has good specificity for identifying IPP.

Keywords Magnetic resonance cholangio-pancreatography · PDAC · Inflammatory pancreatic pseudomass · Duct-interrupted sign · Corona Sign · Attraction Sign

Introduction

Accurate differentiation between inflammatory pancreatic pseudomasses (IPP) and pancreatic ductal adenocarcinoma (PDAC) is fundamental to a patient's management and prognosis. Radiologists may often encounter lesions that show focal enlargement and distortion of the normal contour of the pancreatic head, simulating the appearance of pancreatic cancer, but without any of the pathognomonic features to confirm the diagnosis. A subset of these cases will represent IPP that may be incorrectly managed if not accurately diagnosed [1–4]. Despite clinical symptomatology and biochemical abnormalities that may suggest chronic pancreatitis changes or acute pancreatic inflammation, the certainty of diagnosing the mass as IPP versus PDAC may not be established by clinical history and laboratory values alone. Moreover, although tumor markers CA19-9 and SPan-1 are acknowledged to be somewhat specific in the

✉ Alexander Brook
alejandrogarcesmd@gmail.com

[1] Division of Body MRI, Department of Radiology, Beth Israel Deaconess Medical Center, 330 Brookline Avenue, Boston, MA 02115, USA

confirmation of PDAC, elevation of these markers has also been observed in IPP [5]. Thus, in the absence of or prior to histopathological confirmation, differentiation between IPP and PDAC by imaging diagnosis may play a significant role in the management of these patients, especially since the treatment choice may range from invasive surgical resection for PDAC to pharmacological management for IPP [6, 7].

Multidetector-row computed tomography (MDCT) complemented by endoscopic ultrasound (EUS) and fine-needle aspiration (FNA) plays an important role in diagnosing pancreatic masses. EUS and FNA, however, may not always render an accurate diagnosis as a single sample of inflammatory tissue cannot be used to exclude the presence of carcinoma due to potential sample bias where the malignancy may have been missed. In cases where MDCT, EUS, and FNA are non-diagnostic, MRI with magnetic resonance cholangio-pancreatography (MRCP) has been shown to have increased specificity over MDCT and can play a crucial role as a secondary imaging test [3, 8–11]. MRCP, in the setting of pancreatic mass evaluation, is already widely used and some studies have shown the utility and specificity of MRCP in this context, most notably with the use of the "duct-penetrating" sign that was described and evaluated in 2001. Indeed, this sign was reported to have high specificity for diagnosing IPP [3, 5, 12].

Based on personal experience, we believe that three additional and unexplored MRCP signs might also aid in distinguishing PDAC from IPPs. Firstly, we recognized that most cases with an interrupted and obstructed duct most likely represented neoplastic disease, and have coined it the "duct-interrupted" sign. Secondly, we introduced the "corona" sign defined as dilated side-branches found solely surrounding the pancreatic cancer, alike a crown, and not within in the mass, as can be seen in IPP. Lastly, we aimed to evaluate the "attraction" sign, defined as an approximation of the common bile duct (CBD) to the pancreatic head mass, evidenced by angulation of the obstructed duct towards the mass, which was thought to be highly indicative for IPP.

The purpose of our study was, therefore, to determine the utility of the "duct-interrupted," "corona," and "attraction" signs for the differentiation of PDAC from IPP in the pancreatic head using MRCP.

Materials and methods

Subjects

Institutional review board approval was obtained for this retrospective and Health Insurance Accountability and Probability Act compliant study; requirement for written informed patient consent was waived.

A search of our computerized institutional MRI database was performed to identify all exams between February 2003 and June 2016. Among those, we isolated all cases of solid masses in the head of the pancreas noted in the exam report using the keywords: "focal pancreatitis," "inflammatory mass," "pancreas head," and "pancreatic (ductal) (adeno) carcinoma (PDAC)." The results from this query were then individually evaluated by a single radiologist (K. J. M.) who confirmed the presence of an underlying pancreatic head mass and that all patients underwent MRCP. The search yielded a total of 120 studies initially. However, additional cases were excluded because the MRCP was of insufficient quality ($n = 28$), a metallic stent in the common bile duct was present ($n = 20$), there was variant pancreatic ductal anatomy ($n = 8$), the mass was predominantly cystic rather than solid ($n = 4$); and for other single miscellaneous reasons, including prominent sphincter Oddi complex ($n = 1$), enlarged peripancreatic lymph node ($n = 1$), walled off necrosis ($n = 1$), acute hemorrhagic pancreatitis ($n = 1$), and focal heterogenous enhancement ($n = 3$).

A total of 53 pancreatic head masses were included in our final study group (33 men and 20 women; mean age 55 years ± 18.2 (standard deviation) with age range of 17–87 years. Of those, 17 (32%) were pathologically proven PDACs (ten men and seven women; patient's age ranged between 51 and 87 years (mean, 56 years). The remaining 36 cases (68%) were diagnosed as IPP (23 men and 13 women; patient's age ranged between 17 and 87 years (mean, 55 years). Diagnosis of IPP was based on histopathology ($n = 13$), elevated IgG4 levels ($n = 3$), and/or mean reduction of at least 50% of the size/complete resolution of the mass at follow-up imaging within 1 year from diagnoses ($n = 20$).

MRCP technique

All patients were instructed to fast for 4 h prior to the MRI examination. Images were acquired with a 1.5 or 3 Tesla magnet (Siemens Avanto, Siemens Espree, Siemens Aera or GE Signa HDx) with a phase-array torso coil. The imaging protocol varied, as examinations spanned over 13 years, but all examinations included axial and coronal T2-weighted images (4–6 mm, TR 4000–6000, TE 90–100), thick-slab, heavily T2-weighted MRCP images obtained in oblique coronal plane (40–50 mm, TR 4500, TE 500–700), and thin-section respiratory-triggered or navigator three-dimensional fat-suppressed turbo spin-echo (3D FS TSE) MRCP images obtained in the oblique coronal plane (1–3 mm, TE 150–200, overlap 0–50%). Additionally, T1-weighted three-dimensional fat-suppressed spoiled gradient-echo (T1 FS GRE) and axial T1-weighted 3D dual-echo image (T1 3D dual-echo) (field of view, 320–400 mm; matrix, 192 × 160; slice thickness, 2.5 mm; repetition time, 5.77 ms; echo time, 2.77 ms; received bandwidth, 64 kHz; flip angle, 10°)

were obtained pre-contrast administration and in the arterial (20 s), portal venous (70 s), and delayed phase (3 min). Contrast-enhanced imaging occurred after the intravenous injection of gadolinium chelates (either 0.2 mL/kg gadopentetate dimeglumine {Magnevist, Bayer, Wayne, NJ} [$n = 26$] or 0.1 mL/kg of gadobutrol {Gadavist; Bayer, Wayne, NJ} [$n = 27$]).

Image analysis

Three radiologists with specialized training in abdominal radiology (reader 1, reader 2, reader 3 with 10, 5, and 1 years of experience in reading MRCP studies post residency, respectively) independently reviewed each case. They were blinded to the original radiology report and any clinical information. For each lesion, they recorded bidirectional dimensions of the mass on post-contrast late arterial phase axial T1-weighted sequences (T1 FS GRE) as well as signal intensity compared to pancreatic parenchyma on pre-contrast as well as post-contrast late arterial phase T1 FS GRE (hyperintense, isointense, or hypointense). Three signs were assessed during the evaluation with each reader classifying each MRCP sign on the basis of morphologic gradation for each sign (Figs. 1, 2, 3). The "duct-interrupted" sign was deemed positive for PDAC if the duct within the mass demonstrated complete interruption with upstream dilation (type 5). All other instances where the MPD was present penetrating the mass, for example a normal MPD (type 1), a dilated MPD throughout the pancreatic mass in question and upstream to the lesion (type 2), MPD with stenosis inside the mass and no upstream dilation (type 3), and stenosis inside the mass with upstream dilation (type 4), the "duct-interrupted" sign was deemed negative for PDAC.

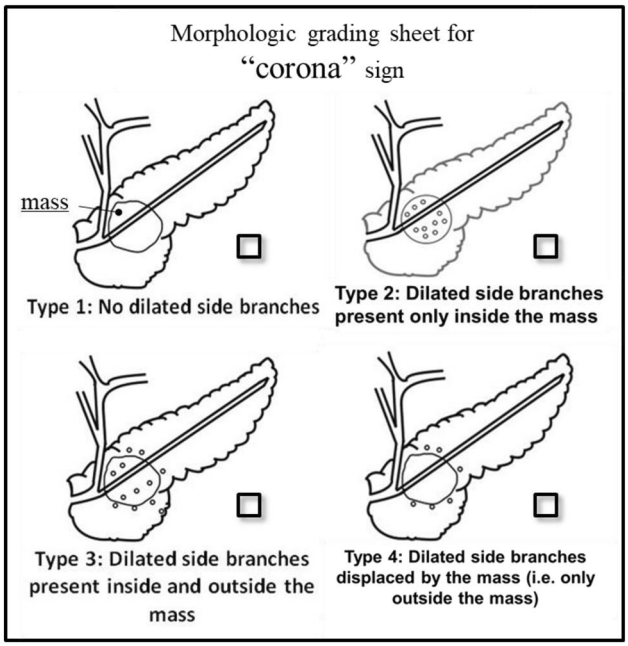

Fig. 2 Morphologic grading sheet for the assessment of the "corona" sign

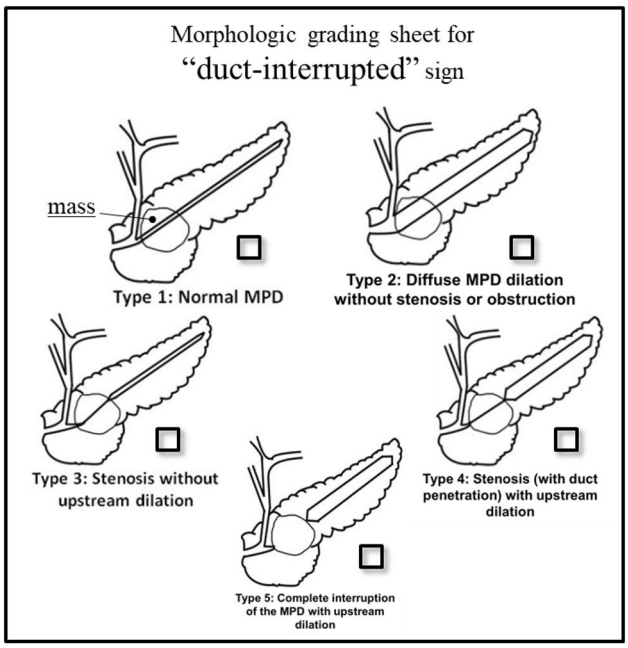

Fig. 1 Morphologic grading sheet for the assessment of the "duct-interrupted" sign

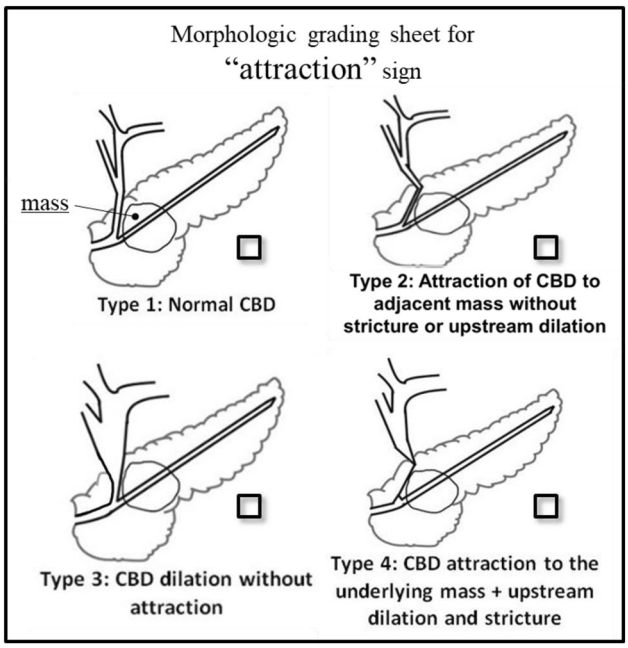

Fig. 3 Morphologic grading sheet for the assessment of the "attraction" sign

The "corona" sign was considered positive for PDAC if dilated side-branches were located exclusively outside of the underlying mass (type 4). In the event that dilated side-branches were not present (type 1), dilated side-branches were present solely inside the mass (type 2), or dilated side-branches were present simultaneously inside and outside the mass (type 3), the "corona" sign was deemed negative for PDAC.

The "attraction" sign was deemed positive for IPP if the dilated CBD showed attraction to the pancreatic mass (type 4), as demonstrated by angulation and formation of a vertex pointing to the underlying mass and simultaneous CBD narrowing and upstream dilation. In the event there was a normal CBD present (type 1), if the common bile duct showed attraction to the mass without CBD narrowing and upstream dilation (type 2), or dilation of the CBD without attraction (type 3), the "attraction" sign was deemed negative for IPP. All images were also evaluated by each reader to determine the presence of additional findings of pancreatitis including pseudocysts, peripancreatic fluid, fat stranding, gland atrophy, and ductal abnormalities.

Statistical analysis

The sensitivity, specificity, and positive and negative predictive values of the "duct-penetrating," "corona," and "attraction" signs in helping to differentiate between IPP and PDAC were calculated, with 95% confidence intervals. The differences in mean pancreatic mass signal intensity compared to the pancreatic parenchyma were also evaluated by the Chi-square test. All statistical analyses were performed using statistical software (Stata/IC 14.2 for Mac, 2017; College Station, TX, USA).

The degree of interobserver agreement between the three readers was calculated using chance-corrected κ statistic. A κ statistic greater than 0.75 was considered excellent agreement beyond chance, 0.4–0.75 fair to good agreement, and less than 0.4, poor agreement.

Results

A total of 53 pancreatic head masses were analyzed. 17 (32%) were pathologically proven PDAC and 36 (68%) were presumed IPP. The focal IPPs were a result of acute focal pancreatitis in 15 (42%) patients, 10 (28%) were due to chronic pancreatitis, 6 (17%) were due to autoimmune pancreatitis (diagnosed by either by IgG4 levels or response to steroids), and 5 (14%) were due to groove pancreatitis.

Mean mass dimensions, upstream MPD dilation, presence of tail atrophy, and chronic pancreatitis by reader are summarized in Table 1. No significant difference was found between PDAC and IPP in relation to any of these characteristics (all p values ≥ 0.05).

The readers reported a range of 9–11 cases (mean: 9.67, SD ± 1.56) showing the "duct-interrupted" sign ($\kappa = 0.41$); out of those, 5–7 (mean: 7, SD ± 2) were pathologically proven PDACs. A range of 6–17 (mean: 9.34, SD ± 5.77) showed a positive "corona" sign ($\kappa = 0.4$); out of those, 5–9 (mean: 6.67, SD + 2.08,) were pathologically proven PDACs. Finally, a range of 11–14 (mean: 12.33, SD ± 1.53) showed a positive "attraction" ($\kappa = 0.54$) and out of those, 7–9 (mean: 8.33, SD ± 1.15) were diagnosed as IPPs.

Table 1 Measurements of pancreatic characteristics by each reader

	Pancreatic measurements and radiological characteristics by pathological diagnosis and by reader[a]		
	Reader 1	Reader 2	Reader 3
PDAC ($n = 17$)			
Antero posterior axis (mm), mean ± SD	21.1 ± 6.02	21.6 ± 6.97	20.3 ± 6.28
Transversal axis (mm), mean ± SD	22 ± 6.57	20.9 ± 6.40	20.9 ± 6.38
Upstream MPD dilation (mm), mean ± SD	6.73 ± 2.15	5.09 ± 1.72	6.43 ± 4.53
Tail atrophy, no (%)	11 (64.7)	10 (58.8)	8 (47)
Chronic pancreatitis, no (%)	12 (70.5)	8 (47)	8 (47)
IPP ($n = 36$)			
Antero posterior axis (mm), mean ± SD	23.1 ± 15.9	21.2 ± 12	21.1 ± 12.2
Transversal axis (mm), mean ± SD	24.3 ± 14	22.8 ± 10.4	22.6 ± 12.5
Upstream MPD dilation (mm), mean ± SD	5.5 ± 1.87	9.16 ± 14.2	6.66 ± 1.95
Tail atrophy, no (%)	20 (55.6)	13 (36.1)	22 (61.1)
Chronic pancreatitis, no (%)	20 (55.6)	8 (22.2)	14 (38.9)

PDAC pancreatic ductal adenocarcinoma; *IPP* inflammatory pancreatic pseudomass; *MPD* main pancreatic duct; *SD* standard deviation

[a]Non-significant relationship was found between PDAC and IPP (p values ≥ 0.05)

The specificities, sensitivities, and positive and negative predictive values of the "duct-interrupted" and "corona" signs in distinguishing PDAC from IPPs and the "attraction" sign for distinguishing IPPs from PDAC are presented in Table 2. The "duct-interrupted" sign (Figs. 4, 5) demonstrated an overall specificity that ranged from 89 to 95%, with a sensitivity range of 29–53%, positive predictive value range from 56 to 82%, and negative predictive value range from 73 to 81%. The "corona" sign (Fig. 6) demonstrated an overall specificity that ranged from 81 to 100%, with a sensitivity range of 29–53%, positive predictive value range from 56 to 100%, and negative predictive value range from 75 to 78%. When both "duct-interrupted" and "corona" signs are present, overall specificity ranged from 91 to 100%, with a sensitivity range of 12–24%, positive predictive value range from 40 to 100%, and negative predictive value range from 68 to 72%. Lastly, the "attraction" sign (Figs. 7, 8) demonstrated an overall specificity that ranged from 71 to 82%, with a sensitivity range of 20–25%, positive predictive value range from 64 to 75%, and negative predictive value range from 31 to 34%.

Signal intensity measurements of the mass compared to the pancreatic parenchyma, on either the pre- or arterial phase post-contrast T1-weighted images, did not show a statistically significant relationship with the diagnosis of PDAC (all p values ≥ 0.05). None of the recorded pancreatitis changes showed a significant relation with the diagnosis of IPP (all p values ≥ 0.05).

Table 2 Duct-interrupted, corona, and attraction signs in differentiating PDAC from IPP using MRCP by readers

MR sign	Signs in differentiating pancreatic ductal adenocarcinoma from inflammatory pancreatic pseudomass using MRCP by readers			
	Sensitivity (%)	Specificity (%)	PPV (%)	NPV (%)
Duct-interrupted				
Reader 1	41	94	77	77
Reader 2	29	89	56	73
Reader 3	53	94	82	81
Corona				
Reader 1	35	100	100	77
Reader 2	53	80	56	78
Reader 3	29	97	83	75
Attraction				
Reader 1	25	82	75	34
Reader 2	25	71	64	31
Reader 3	19	77	64	31
Duct-interrupted + corona				
Reader 1	18	100	100	72
Reader 2	12	91	40	67
Reader 3	24	100	100	71

MRCP magnetic resonance cholangio-pancreatography; *PPV* positive predictive value; *NPV* negative predictive value

Discussion

MRCP imaging has been widely used for the possible differentiation of pancreatic masses [1, 3, 4]. In some instances, however, the distinction of IPP from PDAC can be challenging. Herein, we describe two distinct MRCP signs called the "duct-interrupted" and "corona" signs that are specific for the diagnosis of PDAC and one MRCP sign, called the "attraction" sign, specific for the diagnosis of IPP.

For the majority of available imaging techniques, no clear radiologic criteria have been described for differentiating between IPP and PDAC. Indeed, in our study, established MRI features of peripancreatic inflammation, such as peripancreatic fluid and edema, and findings suggestive of chronic pancreatitis, such as main pancreatic duct irregularity, atrophic pancreatic gland, presence of pseudocysts, and enlarged peripancreatic lymph nodes, did not distinguish IPP from PDAC, confirming the results of previous studies [2, 3].

Few prior studies evaluating ultrasound, endoscopic retrograde cholangio-pancreatography, and MRCP have identified specific signs that utilize morphologic changes of the main pancreatic duct in differentiating IPP from PDAC [13–15]. The most characteristic feature that has shown the highest specificity for distinguishing PDAC from IPP was defined as the "duct-penetrating" sign and showed 96% specificity for identifying IPPs [2]. Other more recent studies have utilized advanced data analysis, such as dynamic enhancement color mapping for the differentiation of pancreatic masses, and have shown increased sensitivity and specificity. However, these data analysis techniques require access to advance software not readily available at all institutions [16, 17].

Histologically, IPP contains cells associated with both acute and chronic inflammation, including lymphocytes, plasma cells, myofibroblastic plasma cells and collagen, resulting in a fibrous reaction rather that a neoplastic reaction [18]. PDAC, however, arises from an intraepithelial neoplastic process that grows uncontrollably and displaces all other surrounding structures. Based on this concept, we hypothesized that there may be additional MRCP signs that might differentiate IPP from PDAC. Firstly, we found that complete obstruction of the main pancreatic duct appears to occur in the setting of malignant neoplasia, as has been previously reported [2, 3]; therefore, we decided to test the sensitivity and specificity for identifying PDAC solely by the presence of complete main pancreatic duct obstruction and dilation, inverting the "duct-penetrating" sign for identifying IPP and using the "duct-interrupted" sign to identify PDAC. This sign showed a specificity ranging from 89 to

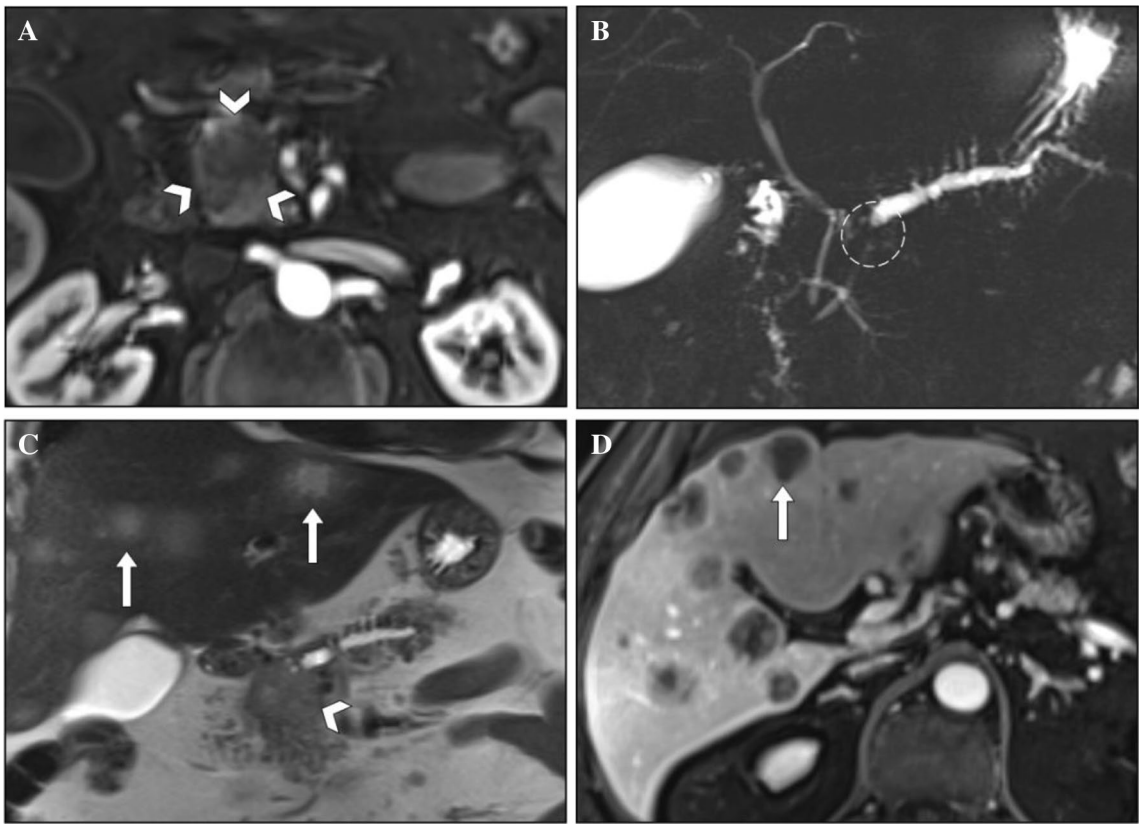

Fig. 4 PDAC with positive "duct-interrupted" sign in a 66-year-old man who presented with abdominal pain and jaundice. **a** Axial fat-suppressed T1-weighted post-contrast image shows hypoenhancing mass in the head of the pancreas (arrowheads). **b** Coronal thick-slab single-shot fast spin-echo MRCP image shows main pancreatic duct interruption at the level of the mass (outline) with dilation of the upstream main pancreatic duct and side-branches. **c**, **d** Coronal T2-weighted and fat-suppressed post-contrast T1-weighted images show multiple metastatic foci (arrows) in liver parenchyma, and pancreatic head mass with duct interruption (arrowhead in C)

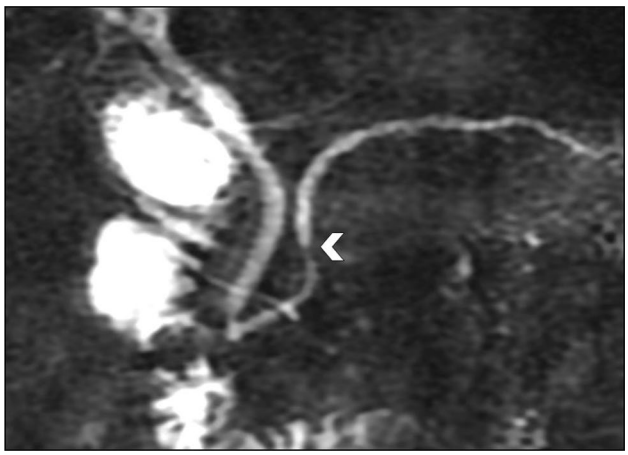

Fig. 5 A 27-year-old woman who presented with chronic pain of unclear etiology. The patient was diagnosed with acute pancreatitis. Coronal thick-slab single-shot fast spin-echo MRCP image shows "duct-penetrating" sign with an abrupt change of caliber of the MPD (arrowhead) and upstream dilation

95%. Secondly, we proposed that in the setting of a malignant process, the mass will occlude side-branches within the mass, and push other dilated side-branches to the periphery of the neoplasm, as opposed to a fibrous reaction where side-branches may not be completely obstructed and may be found inside the inflammatory mass. Given its appearance similar to a crown of dilated side-branches surrounding the mass, this finding was named the "corona" sign which showed specificity for identifying PDAC ranging from 81 to 100%. When both the "duct-interrupted" and "corona sign" were present, the specificity for identifying PDAC increased notably ranging from 91 to 100%. Thirdly, on the basis that peripancreatic inflammation with fibrous reaction causes retraction of adjacent structures rather than invasion as seen in malignant neoplasia, we proposed the "attraction" sign which is defined as attraction of the CBD to the pancreatic mass, demonstrated by angulation and formation of a vertex pointing to the underlying mass. This sign identified IPP with a specificity ranging from 71 to 82%.

The main utility of the three studied signs is to increase specificity of MRI for distinguishing a malignant process

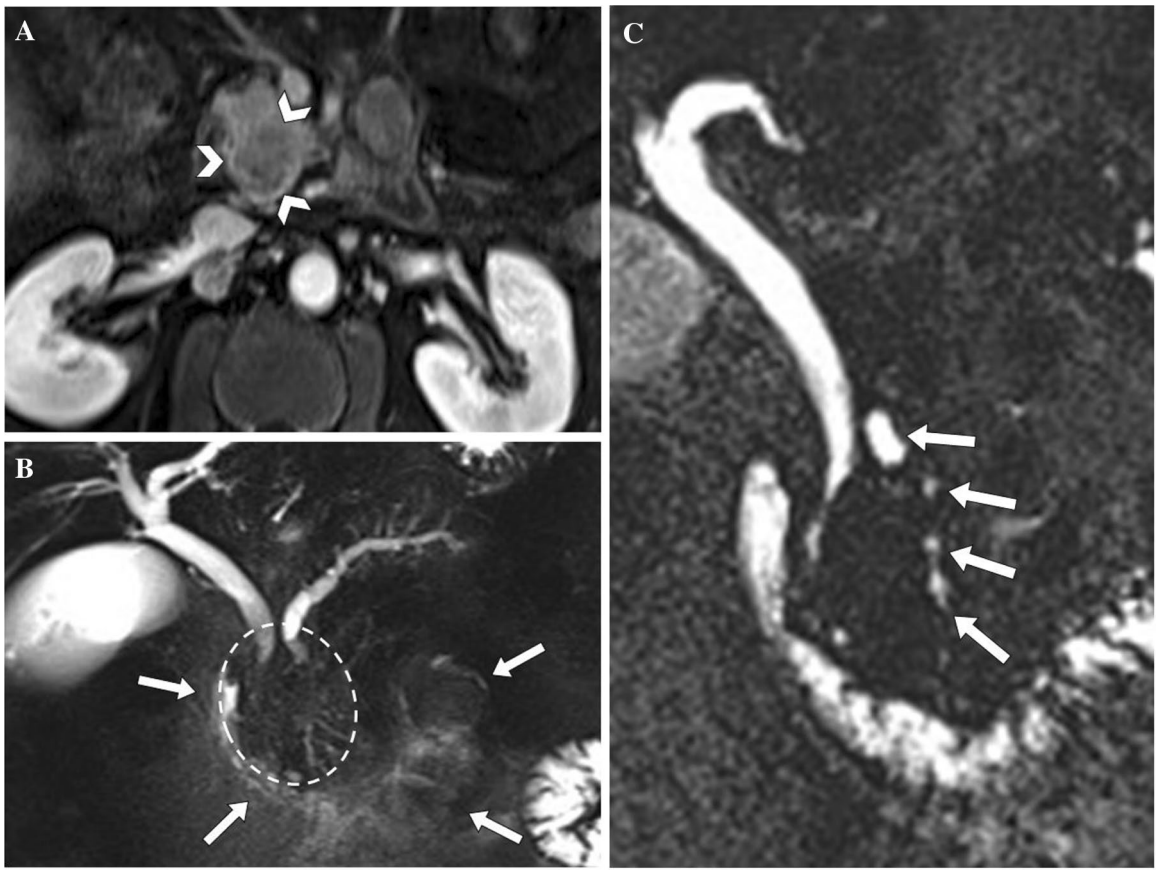

Fig. 6 PDAC with positive "corona" sign in a 61-year-old woman with jaundice. **a** Axial fat-suppressed T1-weighted post-contrast image shows hypointense mass in the head of the pancreas (arrowheads). **b** Coronal thick-slab single-shot fast spin-echo MRCP image shows main pancreatic duct and common bile duct interruption at the level of the mass (outline) with dilation of side-branches outside of the mass only (arrows). **c** MRCP thin-section coronal T2-weighted image shows dilation of side-branches (arrows) alongside a dilated common bile duct

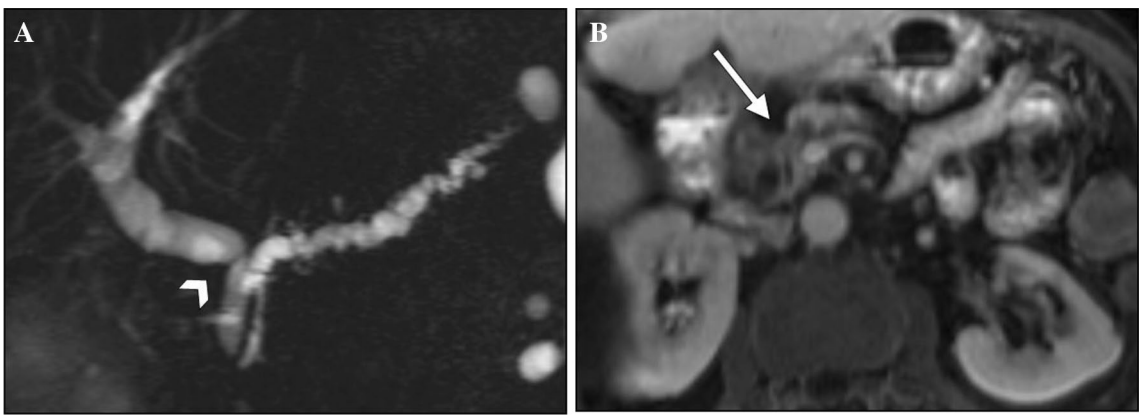

Fig. 7 IPP positive for "attraction" sign in a 77-year-old woman with acute abdominal pain. **a** Coronal thick-slab single-shot fast spin-echo MRCP image shows common bile duct dilation with angulation (arrowhead) and attraction towards the head of the pancreas. Also note "duct penetration" (arrow). **b** Axial contrast-enhanced T1-weighted image shows a hypovascular mass in the head of the pancreas (arrow)

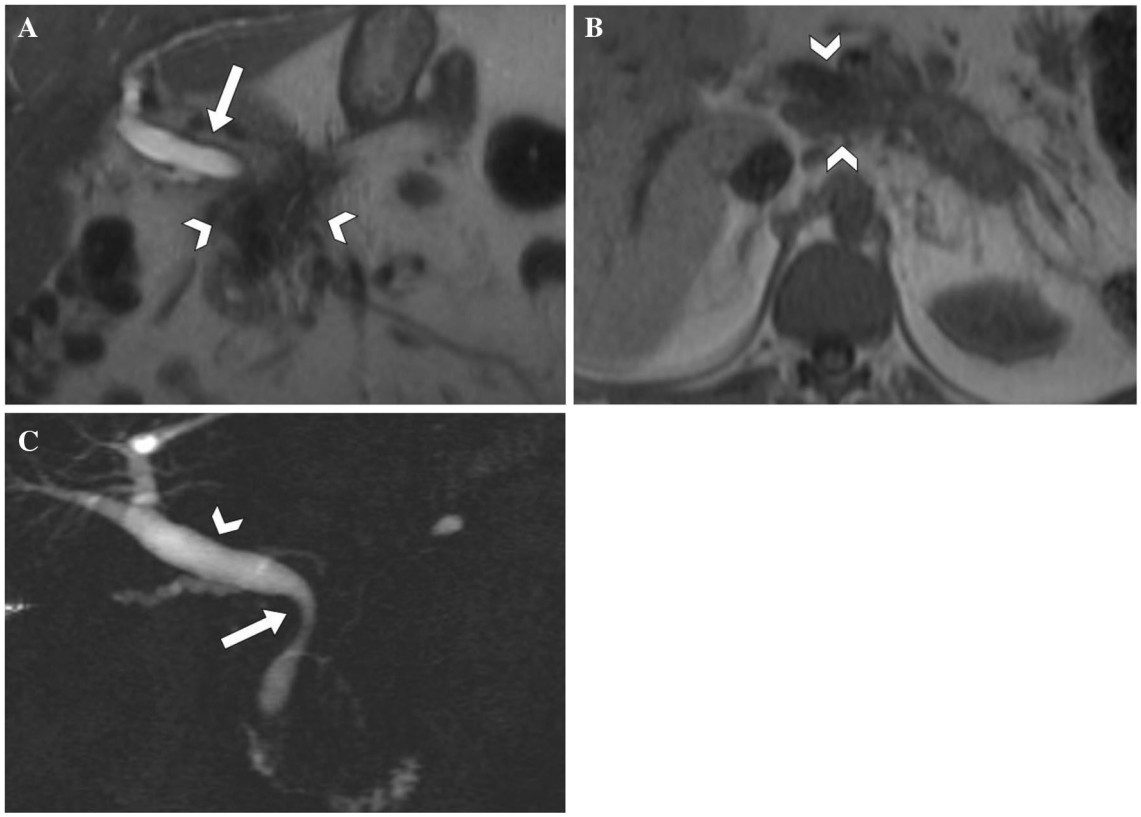

Fig. 8 IPP positive with "attraction" sign in a 35-year-old man with history of chronic pancreatitis. **a** Axial pre-contrast T1 and **b** Axial T2-weighted MR image show a hypointense mass in the head of the pancreas (arrowheads) with CBD dilation (arrow). **c** Coronal thick-slab single-shot fast spin-echo MRCP with attraction of the CBD (arrow) and clear CBD dilation (arrowhead)

from an inflammatory one. MRCP is widely used for characterization of various pathologic pancreatic lesions and increasing quality and information acquired from each MRI study has permitted the detailed characterization of progression of each pathologic process. By identifying common presentations of malignant pathologic process and correlating with known pathophysiology, we were able to successfully increase specificity of MRCP for identifying PDAC and IPP with the use of multiple separate signs. Each sign was individually evaluated and its specificity is not dependent on other findings. Even though the diagrams for each sign had 4–5 morphological types, all data were reviewed as binary positive/negative threshold. We calculated each one against the others, and concluded that morphological type 5 and type 4 were the most specific for PDAC in "duct-interrupted" and "corona" signs, respectively. Also, type 4 in "attraction" sign was the most specific for IPP. This aids in the possible differentiation of multiple pathologic masses regardless of their presentation.

Several limitations regarding our results must be taken into consideration. First, because of the study's retrospective design, there was inevitable selection bias. Secondly, we had pathologic proof in only 13 out of 36 IPPs; however, interval resolution or $\geq 50\%$ reduction in size on follow-up is an accepted method to diagnose IPPs [2]. Thirdly, all masses were located in the head of the pancreas, as this was required to judge the "attraction" sign. The applicability of the two other signs in differentiating pancreatic body or tail PDAC and IPP lesions was therefore not tested. Finally, these findings do not indicate the absolute sensitivity, specificity, or accuracy of these three signs for the prospective diagnosis of PDAC or IPP as this study did not include healthy subjects, and the sample cohort was restricted only to diagnoses of PDAC and IPP.

In conclusion, the "duct-interrupted" sign and "corona" sign have a high specificity for identifying PDAC, while the "attraction" sign has a relatively high specificity for identifying IPP.

References

1. Lee ES, Lee JM. Imaging diagnosis of pancreatic cancer: A state-of-the-art review WJG 20 th Anniversary Special Issues (14): Pancreatic cancer. World J Gastroenterol [Internet]. 2014 [cited 2018 Jan 23];20(24):7864–77. Available from: http://www.wjgnet.com/1007-9327/full/

2. Ichikawa T, Sou H, Araki T, et al. (2001) Duct-penetrating sign at MRCP: usefulness for differentiating inflammatory pancreatic mass from pancreatic carcinomas. Radiology 221(1):107–116
3. Neff CC, Simeone JF, Wittenberg J, Mueller PR, Joseph Ferrucci IT. Inflammatory Pancreatic Masses Problems in Differentiating Focal Pancreatitis from Carcinoma'. [cited 2018 Jan 10]; Available from: http://pubs.rsna.org.ezp-prod1.hul.harvard.edu/doi/pdf/10.1148/radiology.150.1.6689784
4. Schima W, Függer R (2002) Evaluation of focal pancreatic masses: comparison of mangafodipir-enhanced MR imaging and contrast-enhanced helical CT. Eur Radiol. 12:2998–3008
5. Lammer J, Herlinger H, Zalaudek G, Hofler H. Pseudotumorous Pancreatitis. Gastrointest Radiol [Internet]. 1985 [cited 2018 Jan 10];10:59–67. Available from: https://link-springer-com.ezp-prod1.hul.harvard.edu/content/pdf/10.1007%2FBF01893072.pdf
6. Abraham Susan, Wilentz Robb, Yeo Charles, Sohn Taylos, Cameron John, Boitnott John HR. Pancreaticoduodenectomy (Whipple Resections) in Patients Without Malignancy Are They All "Chronic Pancreatitis"? [Internet]. American Journal of Surgical Pathology. 2003 [cited 2018 Jan 10]. p. 110–20. Available from: http://ovidsp.tx.ovid.com.ezp-prod1.hul.harvard.edu/sp-3.27.2b/ovidweb.cgi?WebLinkFrameset=1&S=CGNNFPOMHKDDJKLONCFKKBMCABIBAA00&returnUrl=ovidweb.cgi%3F%26Full%2BText%3DL%257cS.sh.22.23%257c0%257c00000478-200301000-00012%26S%3DCGNNFPOMHKDDJKLONCFKKBMCABIB
7. Kennedy T, Preczewski L, Stocker SJ, Rao SM, Parsons WG, Wayne JD, et al. Incidence of benign inflammatory disease in patients undergoing Whipple procedure for clinically suspected carcinoma: a single-institution experience. [cited 2018 Jan 10]; Available from: https://ac-els-cdn-com.ezp-prod1.hul.harvard.edu/S0002961005009335/1-s2.0-S0002961005009335-main.pdf?_tid=bc50e71a-f61b-11e7-ae4c-00000aacb35d&acdnat=1515598644_1aa840aaa0af7babbcee5f97f76f5cc7
8. Schima W (2006) MRI of the pancreas: tumours and tumour-simulating processes. Cancer Imaging. 6:199–203
9. Choi S-Y, Kim SH, Kang TW, Song KD, Park HJ, Choi Y-H. Differentiating Mass-Forming Autoimmune Pancreatitis From Pancreatic Ductal Adenocarcinoma on the Basis of Contrast-Enhanced MRI and DWI Findings. Am J Roentgenol [Internet]. 2016 Feb [cited 2016 Aug 3];206(2):291–300. Available from: http://www.ajronline.org/doi/10.2214/AJR.15.14974
10. Chen FM, Ni JM, Zhang ZY, Zhang L, Li B, Jiang CJ. Presurgical evaluation of pancreatic cancer: A comprehensive imaging comparison of CT versus MRI. Am J Roentgenol. 2016;
11. Griffin N, Charles-Edwards G, Grant LA (2012) Magnetic resonance cholangiopancreatography: The ABC of MRCP. Insights into Imaging 3:11–21
12. Kim HJ, Kim YK, Jeong WK, Lee WJ, Choi D (2015) Pancreatic duct "Icicle sign" on MRI for distinguishing autoimmune pancreatitis from pancreatic ductal adenocarcinoma in the proximal pancreas. Eur Radiol. 25(6):1551–1560
13. Massey LA, Jäger HR, Paviour DC, O 'sullivan SS, Ling H, Williams DR, et al. The midbrain to pons ratio. [cited 2018 Jun 8]; Available from: https://www.ncbi.nlm.nih.gov/pmc/articles/PMC3908351/pdf/WNL205033.pdf
14. Corwin MT, Gerscovich EO, Lamba R, Wilson M, McGahan JP. Differentiation of Ovarian Endometriomas from Hemorrhagic Cysts at MR Imaging: Utility of the T2 Dark Spot Sign. Radiology [Internet]. 2014;271(1):126–32. Available from: http://pubs.rsna.org/doi/10.1148/radiol.13131394
15. Genders TSS, Spronk S, Stijnen T, Steyerberg EW, Lesaffre E, Hunink MGM. Methods for calculating sensitivity and specificity of clustered Data: A Tutorial 1. Radiol n Radiol [Internet]. 2012 [cited 2018 Jun 8];265. Available from: http://radiology.rsna.org/lookup
16. Negrelli R, Manfredi R, Pedrinolla B, Boninsegna E, Ventriglia A, Mehrabi S, et al. Pancreatic duct abnormalities in focal autoimmune pancreatitis: MR/MRCP imaging findings. Eur Radiol [Internet]. 2015 [cited 2016 Aug 3];25(2):359–67. Available from: http://www.ncbi.nlm.nih.gov/pubmed/25106489
17. Kim M, Mi Jang K, Kim J-H, Kyoung Jeong W, Hyun Kim S, Wook Kang T, et al. Differentiation of mass-forming focal pancreatitis from pancreatic ductal adenocarcinoma: value of characterizing dynamic enhancement patterns on contrast-enhanced MR images by adding signal intensity color mapping. Eur Radiol. 2017;27:1722–1732
18. Patnana M, Sevrukov AB, Elsayes KM, Viswanathan C, Lubner M, Menias CO. Inflammatory pseudotumor: The great mimicker. Am J Roentgenol. 2012;198(3):W217–W227